PHYSICAL REVIEW C VOLUME 25, NUMBER 1 JANUARY 1982

Inelastic electron scattering form factors for the excitation of the 2^+ states in the $1f_{7/2}$ nuclei

Tatsuya Iwamoto* and Hisashi Horie
Department of Physics, Tokyo Institute of Technology, Meguro-ku, Tokyo 152, Japan

Atsushi Yokoyama
Physics Laboratory, School of Medicine, Teikyo University, Hachioji, Tokyo 192, Japan
(Received 23 April 1981)

Coulomb form factors for the $0^+_{gnd} \rightarrow 2^+$ transitions in the even-even $1f_{7/2}$-shell nuclei are studied in terms of the shell model within the $f^n_{7/2} + f^{n-1}_{7/2} p_{3/2}$ configurations and with the effective interactions. It is shown that the characteristics of the $C2$ form factors in the higher-momentum-transfer region, not explained by the simple $f^n_{7/2}$ model, can be interpreted by the mixing of the one-particle excitations into the $p_{3/2}$ orbit in the shell-model wave functions. $E2$ transition strengths and Q moments are also discussed in connection with the $C2$ form factors.

[NUCLEAR STRUCTURE ^{42,44,46,48}Ca, ^{46,48,50}Ti, ^{50,52}Cr, ^{54}Fe; calculated $C2$ form factors for inelastic electron scattering, $B(E2)$ transition strengths and Q moments. Shell model within the $f^n_{7/2} + f^{n-1}_{7/2} p_{3/2}$ configurations with effective interactions.]

I. INTRODUCTION

Electron scattering can provide significant insight into the studies of nuclear structure.[1] By measuring the cross sections for the scattered electrons, one can determine the Fourier transforms of the charge and nuclear-current densities between the initial and final nuclear states. In comparison with ordinary γ transitions, the spatial structure of the nuclear matrix elements can therefore give us a good test of the nuclear wave functions and the transition operators used in the theoretical models.

Experimental data have recently been accumulated on the $0^+_{gnd} \rightarrow 2^+$ transitions in the fp-shell region as well as the higher-multipole transitions.[2-7] Within a measured momentum-transfer range up to $q_{eff} \sim 2.0$ fm^{-1}, there appear two peaks in the $C2$ form factors for the excitation of the first 2^+ states: the first peak appears at $q_{eff} \sim 0.7$ fm^{-1} and the second one appears at $q_{eff} \sim 1.7$ fm^{-1}. For the higher-multipole transitions ($C4$ and $C6$), only a single peak has been observed in a momentum transfer range up to $q_{eff} = 2.0$ fm^{-1}. An interesting feature is the relative magnitude of the first and second peaks observed in the $C2$ form factors. As the simplest interpretation of the $1f_{7/2}$-shell nuclei, we may use the wave functions[8] obtained with the $f^n_{7/2}$ configurations and their appropriate effective interactions. As long as the constant effective charges (q independent) are assumed so as to fit the first peak or the lower-momentum-transfer region of the form factors, one can find systematic deficiencies in the higher-momentum-transfer region; (i) the second peaks are always underestimated by about a factor of 5; and (ii) the calculated positions of the dips are always shifted slightly toward the high-momentum-transfer region. The modification of the radial wave functions may remove the second deficiency but cannot remove the first one. The purpose of the present paper is to show how these deficiencies can be remedied by using the shell-model wave functions[9,10] obtained with the $f^n_{7/2} + f^{n-1}_{7/2} p_{3/2}$ configurations.

In Sec. II, the effective interactions employed in the present calculations are summarized, and the assumptions made in calculating the form factors for inelastic electron scattering are described briefly

for the sake of completeness. The results of our calculations are given and discussed in Sec. III. Our main conclusions are presented in Sec. IV.

II. CALCULATIONS

Shell-model calculations within the $f_{7/2}^n + f_{7/2}^{n-1} p_{3/2}$ configurations have already been made with the effective interaction determined by means of a least-squares fit to selected energy levels.[9,10] We have two parameter sets for the effective interactions that consist of 20 two-body matrix elements and two single-particle energies. One is the calculation by Oda *et al.*,[9] in which the 38 levels chosen from Ca and Sc isotopes ($A=43-48$) were fitted. The other is the calculation by Yokoyama *et al.*,[10] making a χ^2 fitting with the 63 data selected from the $N=27$ and 28 isotones ($A=47-55$). Hereafter, for the sake of simplicity, we refer to cal(Ca-Sc) for the calculations with the former set of effective interactions, and cal(27-28) for that with the latter. It has been revealed from the energy-level calculations that cal(Ca-Sc) works well in the lighter-mass $f_{7/2}$ nuclei, whereas cal(27-28) is better for the heavy ones. Furthermore, the wave functions generally show that the admixture of the $p_{3/2}$ components in the low-lying states is appreciably larger in cal(Ca-Sc) than in cal(27-28). The extent of the admixture seems to be a measure of the deviation from the prediction with the $f_{7/2}^n$ model. The wave functions employed in the present analysis are therefore taken from cal(Ca-Sc) for Ca isotopes and from cal(27-28) for the $N=28$ isotones. Both calculations are presented for the nuclei ^{46,48}Ti and ^{50}Cr. For reference, we make calculations assuming the pure $f_{7/2}^n$ configurations, and the effective interaction for the pure configurations is taken from the empirical energy spectra of ^{48}Sc, by making the Pandya transformation. Although there have been several calculations[8] within the $f_{7/2}^n$ configuration, it would be worth while noting that the wave functions are not sensitive to the effective interactions, as far as the pure configurations are assumed.

Neglecting the transverse scattering of electrons, the cross sections can be described by the Coulomb scattering alone, and further assuming the plane-wave Born approximation (PWBA), the squared form factor $|F|^2$ is given by

$$|F|^2=\frac{4\pi}{Z^2}\frac{1}{2J_i+1}|\langle T_fJ_f||f^{(L)}||T_iJ_i\rangle|^2,$$

where Z is the atomic number of the target nucleus.[1] The wave functions of the initial and the final states are denoted by their isospins and spins: $|T_iJ_i\rangle$ and $|T_fJ_f\rangle$, respectively. The one-particle operator $f^{(L)}$ used in the shell model, is given by

$$f_M^{(L)}=\sum_k e_k j_L(qr_k)Y_M^{(L)}(\Omega_k),$$

where e_k is the charge of the kth nucleon, q is the momentum transfer, j_L is the spherical Bessel function, and $Y_M^{(L)}$ denotes the spherical harmonic of order L. The operator for the ordinary γ transitions is obtained in the limit of $q\to 0$, i.e., $j_L(qr)$ is replaced by r^L.

Since the model space is severely restricted, one should use an effective operator in order to take account of the effects not explicitly included in the assumed model space. In the present calculations, we simply assume constant effective charges e_p and e_n for any protons and neutrons, respectively, which are assigned phenomenologically. In the exact treatment of renormalization in the shell model, the effective charges depend generally on the particle number A, the momentum transfer q, and the states involved in the transitions. To simulate the A dependence as practically as possible, we assign the effective charges to each nucleus so as to reproduce the first peak of the $|F|^2$ or the magnitude of the $|F|^2$ in the lower-momentum-transfer region instead of keeping them unchanged throughout the $1f_{7/2}$ shell.

For the evaluation of the single-particle matrix elements, we use the harmonic oscillator wave functions with the oscillator constant $\nu=0.96\times A^{-1/3}$ fm^{-2}. The center-of-mass correction and the proton-finite-size effect are taken into account by multiplying a factor (Ref. 1)

$$\exp\left[\frac{q^2}{4A}-\frac{a_p{}^2q^2}{4}\right],$$

where $a_p{}^2=0.43$ fm^2. Furthermore, in order to compare the form factors calculated by PWBA with the experimental ones, we use the effective momentum transfer $q_{\rm eff}$ instead of the experimental one q, defined by the relation

$$q_{\rm eff}=q\left[1+\frac{3\sqrt{3}Ze^2}{2\sqrt{5}ER}\right],$$

where R is the rms radius taken from the experiments, and E is the energy of the incident electrons. It is well known empirically, that the Coulomb distortion effect of the scattered electrons are accurately taken into consideration by that relation.

III. RESULTS AND DISCUSSION

A. Ca isotopes

The squared form factors $|F|^2$ for the $0^+_{gnd} \rightarrow 2^+$ transitions in Ca isotopes are calculated and compared with the experiments[2,3] in Fig. 1. The wave functions of the $f^n_{7/2}+f^{n-1}_{7/2}p_{3/2}$ configurations employed in these calculations are obtained from cal(Ca-Sc). Since only the neutrons contribute to the transition matrix elements, their effective charges can therefore be deduced by simply fitting the first peak or the lower-momentum-transfer region of the $C2$ form factors. For ^{46}Ca, however, no electron scattering experiment has been done yet, so that we use the $B(E2)$ value for the $2^+_1 \rightarrow 0^+_{gnd}$ transition to extract the effective charge. The values are then $e_n = 1.7e$, $1.5e$, $0.9e$, and $0.8e$ for ^{42,44,46,48}Ca, respectively, within the $f^n_{7/2}+f^{n-1}_{7/2}p_{3/2}$ configurations. When employing the $f^n_{7/2}$ model, we get $e_n = 1.9e$, $1.7e$, and $1.3e$ for ^{42,44,46}Ca, respectively. The $f_{7/2} \rightarrow f_{7/2}$ transition gives the major contribution to the calculated transition matrix elements of ^{42,44,46}Ca. On the other hand, the 2^+ state of ^{48}Ca consists of the $\nu f_{7/2}{}^7 p_{3/2}{}^1$ component alone, and consequently, the $f_{7/2} \rightarrow p_{3/2}$ transition solely determines the transition matrix element. Comparing with the $f^n_{7/2}$-model predictions for ^{42,44,46}Ca, we obtain the enhancement around the second peaks, and simultaneously, the shift of the dips toward the lower-momentum-transfer region. The $f_{7/2} \rightarrow p_{3/2}$ contributions induced by the $p_{3/2}$ admixture in the 2^+_1 and 0^+_{gnd} wave functions are responsible for these improvements, and the mechanism will be discussed in some more detail for the $N=28$ isotones. The $E2$ properties of the even-mass Ca isotopes including the relevant $B(E2)$ values for the $2^+_1 \rightarrow 0^+_{gnd}$ transitions are calculated by using the same assumptions on the wave functions and effective charges. The results are presented in Tables I and II, and are compared with the experiments.[12–14] It is shown that the data for the γ transitions are consistent with those for the $C2$ form factors. Our calculations for the $|F|^2$ thus reproduce the experiments surprisingly well up to the higher-momentum-transfer region, although it is believed that the admixture of the multiparticle-multihole core-excited deformed states significantly influences the low-lying states in the lighter-mass Ca isotopes (Ref. 11).

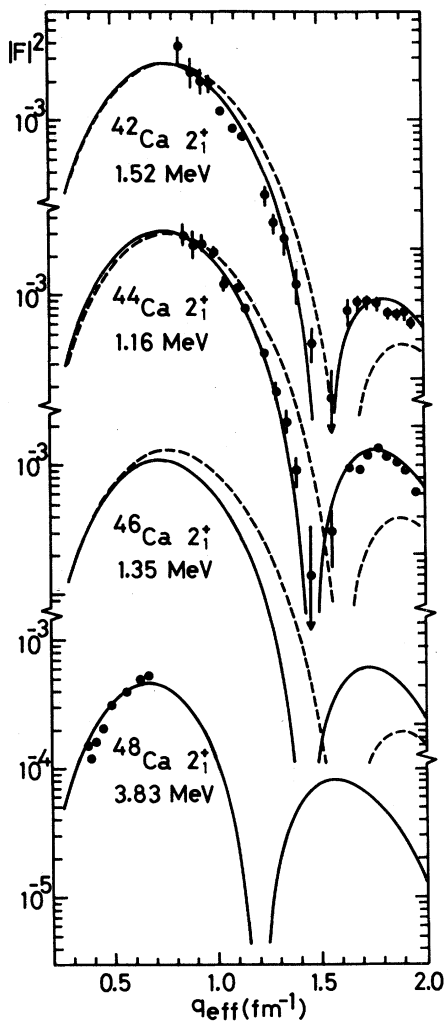

FIG. 1. Experimental and calculated squared form factors $|F|^2$ for the $0^+_{gnd} \rightarrow 2^+_1$ transitions in Ca isotopes. The experimental data denoted by the filled circles are taken from Ref. 2 for ^{42,44}Ca and Ref. 3 for ^{48}Ca. The solid curves show the calculations within the $f^n_{7/2}+f^{n-1}_{7/2}p_{3/2}$ configurations and with the effective residual interactions cal(Ca-Sc). The broken curves denote the $f^n_{7/2}$-model predictions. See the text for the detailed discussion on the effective charges.

B. $N=28$ isotones

The calculated $|F|^2$ for the $0^+_{gnd} \rightarrow 2^+$ transitions in the $N=28$ isotones are shown in Fig. 2 and are compared with the experimental ones.[4–6] The wave functions of the $f^n_{7/2}+f^{n-1}_{7/2}p_{3/2}$ configurations are obtained from cal(27-28), and the calculations with the $f^n_{7/2}$ model are also carried out for reference. In the $f^n_{7/2}$ model, only the protons

TABLE I. $E2$ transition strengths.

Nucleus	J_i	J_f	E_i (MeV)	E_f (MeV)	$B(E2;J_i\rightarrow J_f)(e^2\text{fm}^4)$ Calculation $f^n_{7/2}$	Calculation (Ca-Sc)	Calculation (27-28)	Experiment
^{42}Ca	2	0	1.52	0	72.6	79.0	72.2	83.4±2.8
	4	2	2.75	1.52	72.5	82.2	70.2	65±7
	6	4	3.19	2.75	33.0	50.7	32.2	6.42±0.11
^{44}Ca	2	0	1.16	0	80.0	98.3	75.6	96±7
	4	2	2.28	1.16	88.4	106.1	50.7	>1
	6	4	3.26	2.28	73.8	75.7	37.0	41.2±3.6
^{46}Ca	2	0	1.36	0	36.1	36.1	20.1	35.1±3.6
	4	2	2.58	1.36	36.1	28.3	16.3	
	6	4	2.97	2.58	16.4	3.8	7.9	5.34±0.28
^{48}Ca	2	0	3.83	0		21.0	21.0	19±8[b]
^{46}Ti	2	0	0.89	0	124.0	129.9	119.3	171±8
								214±20
	2	0	2.96	0	1.4	5.2	0.0	$2.0^{+0.6}_{-0.4}$
	2	2	2.96	0.89	47.7	90.4	118.3	180^{+38}_{-35}
	4	2	2.01	0.89	144.0	163.6	127.9	177±20
	6	4	3.30	2.01	125.5	168.0	127.5	150±80
^{48}Ti	2	0	0.98	0	108.8	133.1	110.3	138±12
								150±10
	2	0	2.42	0	6.3	5.6	9.2	$16.2^{+3.8}_{-3.4}$
	2	2	2.42	0.98	101.0	79.9	69.4	$96.8^{+162.4}_{-84.0}$
	4	2	2.29	0.98	135.2	160.7	140.7	100±20
	6	4	3.33	2.29	97.3	132.7	86.7	54±5
^{50}Ti	2	0	1.55	0	65.3	96.3	84.8	66±8
								63±6
	4	2	2.67	1.55	65.2	82.2	75.6	60±12
	6	4	3.21	2.67	29.7	53.4	32.9	33.8±1.2
^{50}Cr	2	0	0.78	0	146.6	256.6	218.9	208±23
								227±20
	2	0	2.92	0	10.0	1.0	6.7	$7.2^{+2.6}_{-2.2}$
	2	2	2.92	0.78	56.3	5.9	16.7	<7.2
	4	2	1.88	0.78	191.7	334.8	285.2	160±20
	6	4	3.16	1.88	162.0	278.4	236.7	130±20
^{52}Cr	2	0	1.43	0	111.7	165.1	144.5	113±10
								132±6
	2	0	2.97	0	0	0.0	4.5	≤0.2
	2	2	2.97	1.43	112.8	146.2	126.1	155^{+31}_{-22}
	4	2	2.37	1.43	123.4	161.7	97.5	83±17

TABLE I. (*Continued.*)

Nucleus	J_i	J_f	E_i (MeV)	E_f (MeV)	$B(E2;J_i\rightarrow J_f)(e^2\text{fm}^4)$ Calculation $f^n_{7/2}$	(Ca-Sc)	(27-28)	Experiment[a]
	4	2	2.77	1.43	0	0.2	26.6	$93.4^{+27.6}_{-24.8}$
	6	4	3.11	2.37	103.1	143.9	75.1	59.5 ± 3.4
	6	4	3.11	2.77	0	2.7	31.1	30.4 ± 4.5
^{54}Fe	2	0	1.41	0	115.1	183.1	138.4	107 ± 8 135 ± 8[c]
	4	2	2.54	1.41	114.9	148.8	95.9	78 ± 16
	6	4	2.95	2.54	52.3	46.5	52.0	40.7 ± 0.7

[a]Experimental data are mostly from the compilation of Reference 12. [b]From Reference 13. [c]From Reference 14.

can contribute to the transition matrix elements, and therefore, we may determine the effective charge for protons by adjusting the first peak of the $C2$ form factors. The values thus obtained are $e_p=1.7e$ for ^{50}Ti, $e_p=1.9e$ for ^{52}Cr, and $e_p=2.2e$ for ^{54}Fe. The $f^n_{7/2}$ model clearly indicates that the $f_{7/2}\rightarrow f_{7/2}$ transition plays a major role in the $|F|^2$, but its contribution alone cannot explain the experimental data in the higher-momentum-transfer region. Within the $f^n_{7/2}+f^{n-1}_{7/2}p_{3/2}$ configurations, since both protons and neutrons can participate in the transition matrix elements, the effective charges may not be uniquely determined by merely fitting the lower-momentum-transfer region of the $|F|^2$. Instead, by taking account of the relevant $E2$ transition strength, and by making the second peak appreciably enhanced, we can obtain the effective charges $e_p=1.4e$ for protons and $e_n=1.0e$ for neutrons in the $0^+_{\text{gnd}}\rightarrow 2^+_1$ transition in ^{50}Ti. The values of e_p and e_n, though not uniquely determined, are consistent with the $E2$ properties of ^{50}Ti, as shown in Tables I and II. The effective

TABLE II. Static quadrupole moments of the first 2^+ excited states.

Nucleus	E (MeV)	$Q(2^+_1)(e\,\text{fm}^2)$ Calculation $f^n_{7/2}$	(Ca-Sc)	(27-28)	Experiment[a]
^{42}Ca	1.52	13.5	−3.5	4.4	-19 ± 8
^{44}Ca	1.16	0	−17.9	−6.4	$-14\ \pm7$
^{46}Ca	1.36	−9.5	−11.3	−10.4	
^{48}Ca	3.83		4.0	4.0	
^{46}Ti	0.89	14.7	−16.7	−0.2	-21 ± 6
^{48}Ti	0.98	3.5	−15.5	−13.1	-19 ± 10 -18 ± 6
^{50}Ti	1.55	12.8	6.6	5.4	-13.5 ± 8.8 8 ± 16 -2 ± 9
^{50}Cr	0.78	−13.5	−30.9	−27.9	$-36\ \pm7$
^{52}Cr	1.43	0	−15.6	−7.2	-14 ± 8
^{54}Fe	1.41	−17.0	−24.3	−24.9	-5 ± 14[b]

[a]Experimental data are mostly from the compilation of Reference 12.
[b]From Reference 14.

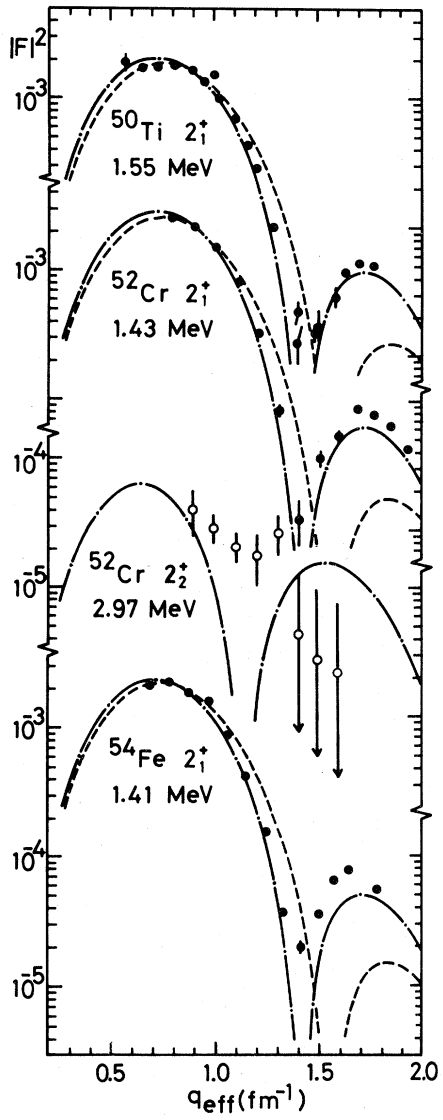

FIG. 2. Experimental and calculated squared form factors $|F|^2$ for the $0^+_{gnd}\rightarrow 2^+_{1,2}$ transitions in the $N=28$ isotones. The experimental data are taken from Ref. 4 for ^{50}Ti, from Refs. 5 and 6 for ^{52}Cr, and Ref. 6 for ^{54}Fe. The filled circles denote the excitation of the 2^+_1 states, while the open circles denote the excitation of the 2^+_2 states. The dotted-dashed curves show the calculations within the $f^n_{7/2}+f^{n-1}_{7/2}p_{3/2}$ configurations with the effective residual interactions cal(27-28). The broken curves describe the $f^n_{7/2}$-model predictions. See the text for the detailed discussion on the effective charges.

charges for ^{52}Cr and ^{54}Fe are taken in such a way that only the isoscalar charge, $\frac{1}{2}(e_n+e_p)$, can be varied so as to fit the lower-momentum-transfer region, while the isovector charge, $\frac{1}{2}(e_n-e_p)$, is kept fixed to that used in ^{50}Ti. The values for protons and neutrons are then $e_p=1.6e$ and $e_n=1.2e$ for ^{52}Cr and $e_p=1.8e$ and $e_n=1.4e$ for ^{54}Fe. Since the 0^+_{gnd} and 2^+_1 states consist mainly of the $f^n_{7/2}$ components, the proton $f_{7/2}\rightarrow f_{7/2}$ transition still gives the major contribution to the form factors. Both proton and neutron excitations can be allowed for the $f^{n-1}_{7/2}p_{3/2}$ configurations, and it turned out that the neutron excitation dominates in the 0^+_{gnd} states, while in the 2^+_1 states it enters into the wave functions roughly twice as much as the proton one does.[10] Although we have several $(f_{7/2})^{n-1}_{T_1\alpha_1 J_1}$ components for the neutron excitation with $T_1=T-\frac{1}{2}$, where T is the isospin defined for the $f^n_{7/2}$ states, there are only a few neutron-excitation components that give sizable contributions to the $C2$ matrix elements for the $0^+_{gnd}\rightarrow 2^+_1$ transitions. Therefore, the $f_{7/2}\rightarrow p_{3/2}$ contributions from neutrons and protons are of comparable magnitude, though the former is still slightly larger than the latter. Since the neutron and proton $f_{7/2}\rightarrow p_{3/2}$ contributions are added in phase in the $C2$ matrix elements for the $0^+_{gnd}\rightarrow 2^+_1$ transitions, the net effects become large enough to give an appreciable correction for the form factors that are dominated by the $f_{7/2}\rightarrow f_{7/2}$ contribution. From the difference in the momentum-transfer dependence between the $(f\,|j_2(qr)\,|f)$ and the $(f\,|j_2(qr)\,|p)$, it is revealed that the $f_{7/2}\rightarrow f_{7/2}$ and the $f_{7/2}\rightarrow p_{3/2}$ contributions are added in phase at $q_{eff}\sim 0.7$ fm^{-1} and at $q_{eff}\sim 1.7$ fm^{-1}, while they are added out of phase at $q_{eff}\sim 1.4$ fm^{-1}. Consequently, we can find that the $f\rightarrow p$ components considerably increase the magnitude of the form factors around their second peaks and shift the positions of the dips toward the lower-momentum-transfer region. The calculations with the $f^n_{7/2}+f^{n-1}_{7/2}p_{3/2}$ model, thus, sufficiently remove the deficiencies that appeared in the $f^n_{7/2}$ model.

The second excited 2^+ state in ^{52}Cr consists mainly of the seniority-4 component of the proton $(f_{7/2})^4$ configuration, and the ground state is dominated by the seniority-0 component of the same configuration. Since the one-particle operator forbids the $\Delta v=4$ transition (the seniority change is 4), the zeroth order $f_{7/2}\rightarrow f_{7/2}$ transition is not allowed. The $f_{7/2}\rightarrow p_{3/2}$ transition, induced by the admixture of the $f^{n-1}_{7/2}p_{3/2}$ components in the wave functions, then becomes important and particularly the neutron contribution dominates in this $0^+_{gnd}\rightarrow 2^+_2$ transition. The calculation shows that the magnitude of the $|F|^2$ for this transition is smaller by about an order of magnitude than that

for the $0^+_{gnd} \rightarrow 2^+_1$ transitions, and the result is comparable with the experiment. Measurements of the $|F|^2$ with further accuracy will be highly anticipated in order to draw a definite conclusion.

C. The nuclei ^{46,48}Ti and ^{50}Cr

Figure 3 compares the calculated with the experimental[2,4,6,7] $|F|^2$ for the $0^+_{gnd} \rightarrow 2^+_{1,2}$ transitions in ^{46,48}Ti and ^{50}Cr. The wave functions of the $f^n_{7/2} + f^{n-1}_{7/2} p_{3/2}$ configurations are obtained from both cal(Ca-Sc) and cal(27-28). Comparison of these two calculations indicates the sensitivity of the form factors to the wave functions. The effective charges in ^{46,48}Ti are taken from those used in ^{50}Ti and those in ^{50}Cr are from ^{52}Cr. For the $f^n_{7/2}$ model, we assume the effective charges $e_p = 1.9e$ and $e_n = 0.9e$, which are taken from Ref. 8. Since both protons and neutrons in the $f_{7/2}$ orbit are active, they both participate in the $f_{7/2} \rightarrow f_{7/2}$ transition. For the $0^+_{gnd} \rightarrow 2^+_1$ transitions, they contribute constructively to the transition matrix elements, whereas they contribute destructively for the $0^+_{gnd} \rightarrow 2^+_2$ transitions. This explains that the magnitude of the $|F|^2$ for the former transitions is larger by an order of magnitude than that for the latter. The same discussion holds, as expected, for the relevant $E2$ transition strengths, as shown in Table I. For the $0^+_{gnd} \rightarrow 2^+_1$ transitions, the $p_{3/2}$ admixture in the wave functions significantly improve the $|F|^2$ in the higher-momentum-transfer region. For the $0^+_{gnd} \rightarrow 2^+_2$ transitions, on the other hand, the $|F|^2$ are rather sensitive to details of the wave functions and the effective charges, since the transition matrix elements are obtained after the complicated destructive interference.

D. $E2$ properties

$E2$ transition strengths and Q moments of the first 2^+ excited states in the $f_{7/2}$ nuclei are calcu-

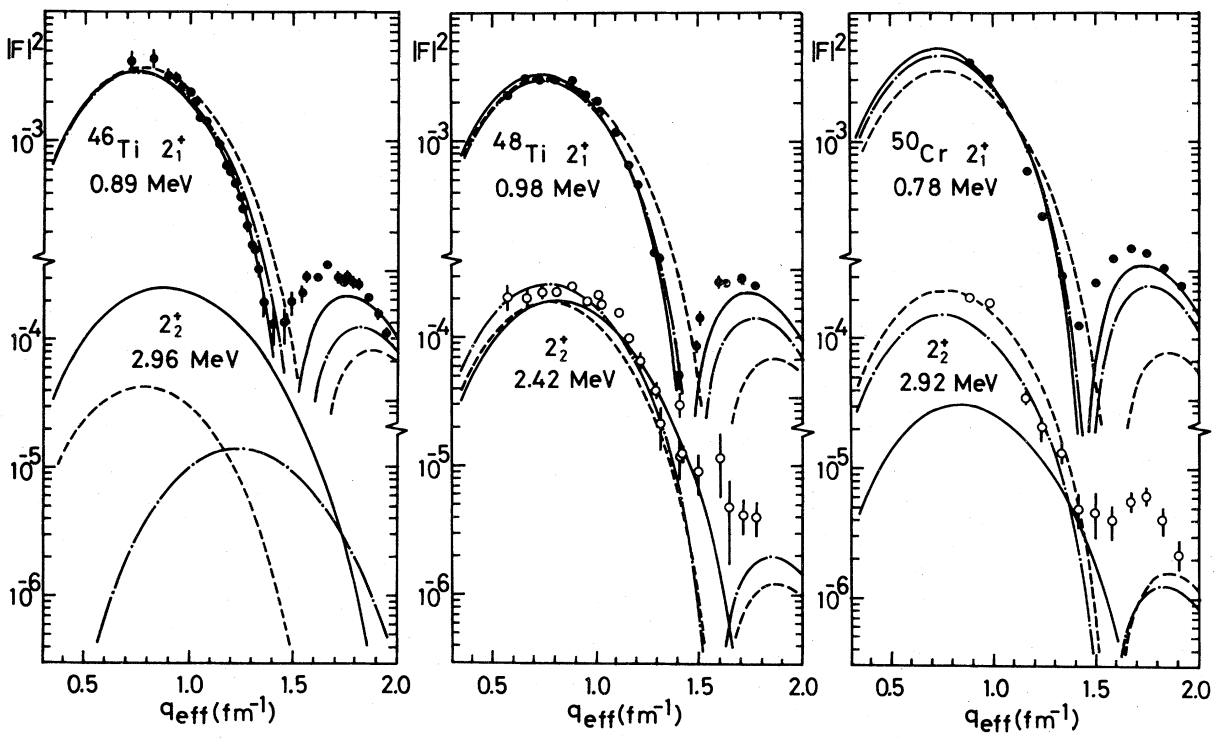

FIG. 3. Experimental and calculated squared form factors $|F|^2$ for the $0^+_{gnd} \rightarrow 2^+_{1,2}$ transitions in ^{46,48}Ti and ^{50}Cr. The experimental data are taken from Ref. 2 for ^{46}Ti, Refs. 4 and 6 for ^{48}Ti, and Ref. 7 for ^{50}Cr. The filled circles denote the excitation of the 2^+_1 states, while the open circles denote the excitations of the 2^+_2 states. The solid and the dotted-dashed curves are obtained with the $f^n_{7/2} + f^{n-1}_{7/2} p_{3/2}$ configurations, using the effective residual interactions cal(Ca-Sc) and cal(27-28), respectively. The broken curves show the $f^n_{7/2}$-model predictions. See the text for the detailed discussion on the effective charges.

lated by employing the same wave functions and the same effective charges as those used in calculating the $C2$ form factors. The results are presented in Table I for $E2$ strengths and in Table II for Q moments, and they are compared with the experimental data recently compiled by Kutschera.[12] The experimental data for ^{48}Ca and ^{54}Fe, taken from Refs. 13 and 14, respectively, are added here to complete the comparison. The results are summarized as follows:

(i) For the transitions that are restricted by a selection rule based on the $f_{7/2}^n$ model, the present calculations with the one-particle excitations considerably remove the defects of the pure configuration assumption. The $E2$ properties of ^{52}Cr may be the typical examples. Within the proton $f_{7/2}{}^4$ configuration outside an inert ^{48}Ca core, the seniority v can be uniquely assigned for each level, and by making the hole-particle conjugation of the wave functions, one can obtain a selection rule indicating that the $\Delta v=0$ transition is strictly forbidden. The Q moment in this nucleus must be, therefore, exactly zero. The experimental value for the $Q(2_1^+)$ is negative and relatively large, being contrary to that prediction. The present calculation with the $f_{7/2}{}^{12}+f_{7/2}{}^{11}p_{3/2}$ configuration, on the other hand, predicts the negative value for the $Q(2_1^+)$, nicely reproducing the experimental one. The same discussion can be applied for ^{44}Ca.

(ii) A distinctive improvement is obtained in the Q moments of the 2_1^+ states in Ti isotopes. For ^{46,48}Ti, the pure configuration assumption gives the positive values for the $Q(2_1^+)$, whereas the negative values are obtained with the $f_{7/2}^n+f_{7/2}^{n-1}p_{3/2}$ configurations, being in agreement with the experiments.

(iii) For other transitions, both the predictions, with and without the one-particle excitations, almost equally reproduce the experiments. Neither model can explain the state dependence of the $E2$ matrix elements observed throughout the $1f_{7/2}$ shell, and it is left to be an open question.

Within the existing experimental uncertainties on the $E2$ data, it thus may be said that the calculations of the $C2$ form factors are consistent with those of the $E2$ properties of the relevant nuclei.

IV. SUMMARY AND CONCLUSIONS

Coulomb form factors for the $0_{\text{gnd}}^+\rightarrow 2^+$ transitions in the $f_{7/2}$ nuclei have been discussed in terms of the shell model within the $f_{7/2}^n+f_{7/2}^{n-1}p_{3/2}$ configurations and with the effective interactions. Two kinds of the effective interactions are used, which were deduced from the different χ^2-fitting procedures. One is obtained from the calculation with Ca and Sc isotopes, and the other from that with the $N=27$ and 28 isotones. In the present calculations of the form factors, the $B(E2)$ values and the Q moments, the former is employed for Ca isotopes, the latter for the $N=28$ isotones and both of these two for ^{46,48}Ti and ^{50}Cr. The constant effective charges are used for the sake of simplicity, although we have to assume the relatively strong number dependence for them. In the excitation of the first 2^+ excited states, the $f\rightarrow f$ and $f\rightarrow p$ contributions, having the different q dependence, interfere constructively and destructively depending on the momentum-transfer range, and therefore, the $p_{3/2}$ admixture in the wave functions enhances the magnitude of the form factors around the second peaks and shifts the positions of the dips toward the lower-momentum-transfer region. It is therefore indicated that the systematic deficiencies of the $f_{7/2}^n$-model predictions can be remedied by the $f_{7/2}^n+f_{7/2}^{n-1}p_{3/2}$ model. Furthermore, the $E2$ properties of the even-even $f_{7/2}$ nuclei are calculated with the same assumptions, and they are shown to be consistent with the electron scattering data. Origin of the effective charges including their strong number dependence, although beyond the scope of the present calculations, will be an important subject to be investigated.

ACKNOWLEDGMENTS

We wish to thank Professor M. Oyamada for communicating to us the experimental data. We also thank Dr. K. Muto, Dr. M. Hino, and Dr. T. Shimano for their help in the numerical calculations. The numerical calculations were carried out with the HITAC M-200H computer system at Tokyo Institute of Technology.

*Present address: NAIG Nuclear Research Laboratory, Nippon Atomic Industry Group Co., Ltd., Kawasaki, Kanagawa 210, Japan.

[1]T. deForest and J. Walecka, Adv. Phys. 15, 1 (1966); H. Überal, *Electron Scattering From Complex Nuclei* (Academic, New York, 1971).

[2]J. Heisenberg, J. S. McCarthy, and I. Sick, Nucl. Phys. A164, 353 (1971).

[3]R. A. Eisenstein, D. W. Madsen, H. Theissen, L. S. Cardman, and C. K. Bockelman, Phys. Rev. 188, 1815 (1969).

[4]A. Hotta, K. Hayakawa, K. Takayama, I. Okazaki, and M. Oyamada, Res. Rep. Nucl. Sci. (Tohoku University) 9, 7 (1976); 10, 18 (1977).

[5]K. Hosoyama, I. Okazaki, M. Oyamada, Y. Torizuka, and K. Arita, Res. Rep. Nucl. Sci. (Tohoku University) 7, 279 (1974); 8, 55 (1975).

[6]K. Hosoyama, A. Hotta, M. Kawamura, T. Nakazato, and M. Oyamada, Res. Rep. Nucl. Sci. (Tohoku University) 11, 1 (1978).

[7]J. W. Lightbody, Jr., *et al.*, Bull. Am. Phys. Soc. 20, 568 (1975).

[8]W. Kutschera, B. A. Brown, and K. Ogawa, Riv. Nuovo Cimento 1, 1 (1978); K. Muto, T. Oda, and H. Horie, Prog. Theor. Phys. 60, 1350 (1978) and references therein.

[9]T. Oda, K. Muto, and H. Horie, Lett. Nuovo Cimento 18, 549 (1977).

[10]A. Yokoyama, T. Oda, and H. Horie, Prog. Theor. Phys. 60, 427 (1978).

[11]G. E. Brown and A. M. Green, Nucl. Phys. 75, 491 (1966); W. J. Gerace and A. M. Green, *ibid.* A93, 110 (1967); and B. H. Flowers and L. D. Skouras, *ibid.* A136, 353 (1969).

[12]W. Kutschera, in Proceedings of the Topical Conference on Physics of Medium-Light Nuclei, Florence, 1977, edited by P. Blasi and R. A. Ricci (Editrice Compositori, Bologna, 1978) p. 120.

[13]J. W. Tape, R. Hensler, N. Benczer-Koller, and J. R. MacDonald, Nucl. Phys. A195, 57 (1972).

[14]M. J. Levine, E. K. Warburton, and D. Schwalm, Phys. Rev. C 23, 244 (1981).